

International Journal of Modern Physics E  
 © World Scientific Publishing Company

## LIGHT EXOTIC NUCLEI WITH EXTREME NEUTRON EXCESS AND $2 \leq Z \leq 8$

V.N. TARASOV<sup>1</sup>, K. A. GRIDNEV<sup>2,3</sup>, V.I. KUPRIKOV<sup>1</sup>, D. K. GRIDNEV<sup>2,3</sup>,  
 D.V. TARASOV<sup>1</sup>, K.S. GODBEY<sup>4</sup>, X. VIÑAS<sup>5</sup> and WALTER GREINER<sup>3</sup>

<sup>1</sup>*NSC, Kharkov Institute of Physics and Technology, Kharkov, 61108 Ukraine*

<sup>2</sup>*Institute of Physics, St. Petersburg State University, St. Petersburg, 198504 Russia*

<sup>3</sup>*Frankfurt Institute of Advanced Studies, Frankfurt am Main, 60438 Germany*

<sup>4</sup>*Vanderbilt University, Nashville, Tennessee 37235, USA*

<sup>5</sup>*University of Barcelona, Barcelona, E-08028 Spain*

Received (received date)

Revised (revised date)

Using HF+BCS method we study light nuclei with nuclear charge in the range  $2 \leq Z \leq 8$  and lying near the neutron drip line. The HF method uses effective Skyrme forces and allows for axial deformations. We find that the neutron drip line forms stability peninsulas at <sup>18</sup>He and <sup>40</sup>C. These isotopes are found to be stable against one neutron emission and possess the highest known neutron to proton ratio in stable nuclei.

### 1. Introduction

Nuclei with extreme neutron excess lying close to the neutron drip line constantly attract interest both in theoretical and experimental research. Experiments with radioactive nuclear beams that are conducted in Dubna, GSI, RIKEN have opened new opportunities for obtaining exotic nuclei with impressive neutron excess. The construction of FRIB in Michigan<sup>1</sup> (the operational run is planned in 2022) would boost experimental abilities to approach the neutron drip line. Among major fundamental microscopic approaches in the studies of nuclei with neutron excess one can name the Hartree-Fock-Bogoliubov approach (HFB), Hartree-Fock plus BCS pairing (HF+BCS) with effective forces and relativistic mean field theory.<sup>2-7</sup>

In Refs. 8, 9, 10, 11, 12, 13, 14, 15 we explored the possibility of existence of islands and peninsulas of stability of nuclei with large neutron excess lying beyond the conventional neutron drip line. The calculations in these papers were done with the HF method using various type of effective Skyrme forces<sup>17-21</sup> and accounting for the axial deformation; the pairing was treated in the BCS scheme. We have demonstrated that in the regions of the nuclear chart corresponding to extreme

neutrons excess around magic and “new” magic numbers  $N = 32, 58, 82, 126, 184, 258$  there may exist peninsulas of neutron stability stretching beyond the conventional neutron drip line. In this picture a neutron rich nucleus, which is unstable against neutron separation, may regain stability if one adds to it a certain number of neutrons thereby shifting it to the stability peninsula. In the HF approach this stability restoration is a result of complete filling of neutron subshells with large angular momentum. These subshells have a large centrifugal barrier and being partially filled they are located in the continuous spectrum, which makes the corresponding nuclei unstable against neutron emission. However, when the neutron number increases these subshells descend into discrete spectrum and nuclei regain stability. The main aim of the present paper is to find stable nuclei with the highest possible neutron to proton ratio  $N / Z$ , which we believe sets a theoretical upper bound for this ratio. We shall consider only nuclei with  $2 \leq Z \leq 8$ , since it has been shown earlier,<sup>11–13</sup> the maximal  $N / Z$  ratio can be attained only for light nuclei. The largest values of  $N$  are obtained at stability peninsulas. The most extended stability peninsulas are obtained with the SkI2<sup>12–14</sup> set of Skyrme forces, therefore, we shall use mostly the SkI Skyrme parameters. Let us note that various types of SkI forces were obtained and effectively used in Ref. 20. The same type of forces was used in Ref. 22 for the description of light exotic nuclei, however, without accounting for deformation, which is, certainly, a disadvantage compromising the predictive power of the obtained results.

## 2. Methods and Results

The detailed exposition of the method of solving the deformed Hartree-Fock (DHF) equations is given in Refs. 9, 23, 24, 25. Here we present the results of the calculations using SkI2 set of Skyrme forces. One particle wave functions in DHF are expanded in the axially deformed harmonic oscillator basis. The principle quantum number for the harmonic oscillator basis usually does not exceed  $N_0 = 18$  (amounting to 1330 basis functions). This dimension of the basis is more than necessary for the calculations of the isotopes with  $2 \leq Z \leq 8$ , which provides high accuracy and reliability of obtained results.

In case of nuclei lying on stability peninsulas along with the DHF calculations we do additional calculations, where HF equations are solved directly in coordinate space under assumption of spherical symmetry (SHF method).<sup>26</sup> This is reasonable because nuclei belonging to stability peninsulas indeed possess spherical symmetry.<sup>8–15</sup> SHF calculations make possible the analysis of the role of continuum states in the cases when the DHF solution is spherically symmetric. We used the BCS constant pairing, where the pairing constant is set equal to  $G = (19.5/(N + Z))[1 \pm 0.51(N - Z)/(N + Z)]$ ,<sup>27</sup> “+” and “-” correspond to protons and neutrons respectively. In DHF calculations pairing is restricted to bound one-particle states. This choice of pairing as well as the role of continuum states in the structure of nuclei lying at stability peninsulas is discussed in Refs. 11, 12, 13,

14, 15. Let us note that the inclusion of continuum states into present SHF calculations of nuclei with  $2 \leq Z \leq 8$ , which form stability peninsula, did not affect the results that were obtained without inclusion of continuum states. This is, however, typical for magic and quasi-magic nuclei. Similar behavior has been observed for stability peninsulas in other parts of the nuclear chart.<sup>13</sup>

Fig. 1 shows nuclear chart, where the squares represent nuclei that are stable against one neutron emission in DHF calculations with SkI2 forces. Exactly the same picture is obtained with SkI1 forces. Grey squares on this chart are experimentally known stable nuclei. We determine one neutron drip line from the condition  $S_n = 0$ , where  $S_n$  denotes one neutron separation energy. Thereby, any positive value of  $S_n$  means stability against one neutron emission, even if  $S_n$  is marginally small. We calculate one neutron separation energies assuming the validity of approximation made in Koopmans theorem. For given  $Z$  the position of the neutron drip line is determined as follows. We start with a stable isotope and increase the neutron number until stability is lost and one neutron separation energy changes its sign. Knowing that one-neutron drip line can exhibit nonmonotonic behavior<sup>13</sup> we continue increasing  $N$ . If at some larger value of  $N$  the value of  $S_n$  changes its sign again then this means that we have located a stability peninsula. As we have mentioned such effect of stability restoration appears when neutron subshells with large angular momentum getting fully filled intrude from continuous spectrum into the bound spectrum.<sup>11-15</sup> (In<sup>16</sup> the formation of stability peninsulas was alternatively termed irregular behavior of the neutron drip line). Using SkI2 set of Skyrme forces we have found one stability peninsula situated at <sup>18</sup>He with the fully filled subshell  $1d_{5/2}$  and another one at <sup>40</sup>C with the fully filled subshell  $1f_{7/2}$ . These isotopes that disrupt the monotonic behavior of the drip line are illustrated in Fig. 1, where they are highlighted with red (color online) color and have arrows pointing at them. Both of these nuclei possess spherical symmetry, which is typical for nuclei with fully filled shells. The neutron to proton ratio in <sup>18</sup>He and <sup>40</sup>C is  $N/Z = 8$  and  $N/Z \simeq 5.67$  respectively, which is substantially larger than the so far known neutron to proton ratios for stable nuclei.<sup>9-15</sup> Fig.1 also shows the stability peninsula consisting of one isotope <sup>32</sup>C. Later we shall discuss in detail the stability restoration for this isotope.

Fig. 2 shows one neutron separation energies as functions of  $A = (Z + N)$  obtained with SkI2 Skyrme forces. One can clearly see  $S_n$  changing sign at <sup>18</sup>He, which results from completely filled subshell  $1d_{5/2}$  being bound. One neutron separation energy of this isotope as estimated according to the Koopmans theorem equals 0.45 MeV. Let us consider HF potentials corresponding to the state  $1d_{5/2}$ , where this state is weakly bound. Because the nucleus is spherical we can use SHF method, which has the advantage of representing potentials and wave functions directly in coordinate space.<sup>11,26</sup> The DHF value  $S_n = 0.450$  is close to the SHF value  $S_n = 0.406$  MeV. Fig. 3 shows the Fermi level  $1d_{5/2}$  for <sup>18</sup>He and the corresponding SHF potential. The dotted line depicts the wave function of the Fermi level, which is localized under the centrifugal barrier. The height of the centrifugal barrier in the

HF potential equals 1.35 MeV, which should additionally enhance the stability of  $^{18}\text{He}$  against one neutrons emission. When we apply the BCS scheme in case of SHF calculations we also include those localized quasibound states with positive energy, whose wave functions are localized under the centrifugal barrier. Other continuum states are not considered. In case of  $^{18}\text{He}$  and  $^{40}\text{C}$  (SkI2 forces) we considered all localized quasibound states. The states were discretized by introducing boundary conditions, which make wave functions vanish outside the sphere with the radius 40 fm. We found that the pairing remained zero even when we included localized quasibound states.

Fig. 4 shows one neutron separation energies for carbon calculated with SkI2 forces using the DHF method. One can see that  $S_n$  increases for  $A = 26$ , which signals the magicity of the number  $N = 20$  near the drip line. The neutron subshell  $1f_{7/2}$  submerses into bound spectrum becoming completely filled for  $N = 34$ , which provides stability against one neutron emission for  $^{40}\text{C}$ . At this point  $S_n = 0.597$  MeV in DHF calculations and  $S_n = 0.594$  MeV in SHF calculations.  $^{40}\text{C}$  is a spherically symmetric nucleus. Similar to the case of  $^{18}\text{He}$  in Fig. 5 we consider the SHF potential corresponding to the Fermi level  $1f_{7/2}$  for  $^{40}\text{C}$ . The SHF potential for this state has a centrifugal barrier with the height 2.48 MeV, which additionally enhances the stability of this isotope. In Fig. 4 one witnesses the stability restoration for  $^{32}\text{C}$  (26 neutrons), which is again connected with the state  $1f_{7/2}$ . Unlike  $^{40}\text{C}$  the nucleus  $^{32}\text{C}$  has quadrupole deformation  $\beta = -0.32$ , and its last filled neutron level has quantum numbers  $\Omega = 7/2^-$ . This level, which is the member of the multiplet  $1f_{7/2}$ , intrudes into the bound part of the spectrum when  $N = 26$ .

Let us consider in more detail the isotope chains of He and C, which pass through  $^{18}\text{He}$  and  $^{40}\text{C}$ . In Figs. 6, 7 one can see the neutron and proton root mean square (rms) radii  $\langle r_{n,p}^2 \rangle^{1/2}$  for helium and carbon. The arrows indicate the values for  $^{18}\text{He}$  and  $^{40}\text{C}$ , which form stability peninsulas at  $N = 16$  and  $N = 34$ . Generally in neutron rich nuclei the difference of neutron and proton rms radii  $\Delta R_{n,p} = \langle r_n^2 \rangle^{1/2} - \langle r_p^2 \rangle^{1/2}$  may take large values and one can speak about neutron skin or neutron halo effects when  $\Delta R_{n,p} > 0.2$  fm.<sup>28</sup> From the figure one can see large values of  $\Delta R_{n,p}$  for He and C isotopes in particular for  $^{18}\text{He}$  and  $^{40}\text{C}$ , which is a manifestation of a large neutron halo in these nuclei. In DHF calculations for  $^{18}\text{He}$  we obtained  $\Delta R_{n,p} = 4.288 - 2.150 = 2.138$  fm and  $\langle r_n^2 \rangle^{1/2} / \langle r_p^2 \rangle^{1/2} \simeq 1.994$ . For  $^{40}\text{C}$  we got  $\Delta R_{n,p} = 4.709 - 2.800 = 1.909$  fm and  $\langle r_n^2 \rangle^{1/2} / \langle r_p^2 \rangle^{1/2} \simeq 1.682$ . It is useful to compare these values with those of extremely neutron rich  $^{40}\text{O}$ ,<sup>29</sup> where  $\Delta R_{n,p} = 1.29$  fm and  $\langle r_n^2 \rangle^{1/2} / \langle r_p^2 \rangle^{1/2} \simeq 1.436$  (SkM\* forces). This suggests that there is a very large neutron halo in  $^{18}\text{He}$  and  $^{40}\text{C}$  in the picture corresponding to SkI2 forces.

Figs. 8, 9 show neutron and proton density distributions of  $^{18}\text{He}$  and  $^{40}\text{C}$  calculated within SHF approximation using SkI2 forces. SHF approximation yields the wave function in coordinate representation and is thus more appropriate for graphical purposes. Its use in this case is justified by the spherical form of these nuclei. Neutron halo in neutron rich nuclei is first of all characterized by the spatially ex-

tended neutron density distribution dominating over the “normal” proton density distribution. In this sense Figs. 8, 9 provide a more clear picture of neutron halo in nuclei forming stability peninsulas. Neutron and proton density distributions in Figs. 8, 9 are typical for neutron rich nuclei.<sup>7</sup> Our analysis shows that the tail of neutron distribution results from weakly bound one particle states.

### 3. Conclusion

We did HF + BCS calculations of neutron rich nuclei with charges  $2 \leq Z \leq 8$ . We have demonstrated that beyond conventional neutron drip line there may exist stability peninsulas formed by <sup>18</sup>He and <sup>40</sup>C. These nuclei set the record for the largest so far known neutron to proton ratio for stable nuclei. They are spherical in shape and have a spatially extended neutron halo. These newly found stability peninsulas complement our previous findings and their existence agrees with the general nature of the neutron drip line forming peninsulas at magic and quasimagic neutron numbers.

### References

1. J. Wei, Proceedings of PAC2013; Pasadena, CA, USA; September 29- October 4, 2013, pp. 1453-1457; see also <http://frib.msu.edu/about>
2. M. Bender, P.-H. Heenen and P.-G. Reinhard, Rev. Mod. Phys. **75** (2003) 121.
3. M.V. Stoitsov *et al.*, Phys. Rev. C **61** (2000) 034311.
4. M.V. Stoitsov *et al.*, Phys. Rev. C **68** (2003) 054312; <http://www.fuw.edu.pl/~dobaczew/thodri/thodri.html>
5. S. Hilaire and M. Girod, Eur. Phys. J. A **33** (2007) 237.
6. N. Tajima, Progr. Theor. Phys. Supl. **142** (2001) 265.
7. J. Meng *et al.*, Prog. Part. Nucl. Phys. **57** (2006) 470.
8. K.A. Gridnev *et al.*, Eur. Phys. J. A **25** S01 (2005) 353.
9. K. A. Gridnev *et al.*, Int. J. Mod. Phys. E **15** (2006) 673.
10. V.N. Tarasov *et al.*, Int. J. Mod. Phys. E **17** (2008) 1273.
11. V.N. Tarasov *et al.*, Phys. Atom. Nucl. **75** (2012) 17.
12. V.N. Tarasov *et al.*, Bull. Russ. Acad. Sci. Phys. **76** (2012) 876.
13. V.N. Tarasov *et al.*, Int. J. Mod. Phys. E **22** (2013) 1350009.
14. V.N. Tarasov *et al.*, Bull. Russ. Acad. Sci. Phys. **77** (2013) 842.
15. V.N. Tarasov *et al.*, Bull. Russ. Acad. Sci. Phys. **78** (2014) 569.
16. J. Erler, N. Birge, M. Kortelainen, W. Nazarewicz, E. Olsen, A.M. Perhac and M. Stoitsov, Nature **486** (2012) 509.
17. H.S. Khler, Nucl. Phys. A **258** (1976) 301.
18. J. Bartel *et al.*, Nucl. Phys. A **386** (1982) 79.
19. E. Chabanat *et al.*, Nucl. Phys. A **635** (1998) 231; Erratum-ibid **643** (1998) 441.
20. P.-G. Reinhard and H.Flocard, Nucl. Phys. A. **584** (1995) 467.
21. J. Dobaczewski *et al.*, Nucl. Phys. A **422** (1984) 103.
22. Yao-Song Shen, Zhong-Zhou Ren, Commun. Theor. Phys. **35** (2001) 563.
23. D. Vautherin and D.M. Brink, Phys. Rev. C **5** (1972) 626.
24. D. Vautherin, Phys. Rev. C **7** (1973) 296.
25. V.N. Tarasov *et al.*, Preprint **85-32** HFTI (CNII Atominform, Moscow, 1985).
26. E.V. Inopin, V.Yu. Gonchar and V.I. Kuprikov, Yad. Fiz. **24** (1976) 40; Sov. J. Nucl. Phys. **24** (1977) 20.

6 *V. N. Tarasov et al.*

27. V.E. Mitroshin, Phys. Atom. Nucl. **68** (2005) 1314.
28. S. Mizutori *et al.*, Phys. Rev. C **61** (2000) 044326.
29. K.A. Gridnev *et al.*, Bull. Russ. Acad. Sci. Phys. **76** (2012) 871.

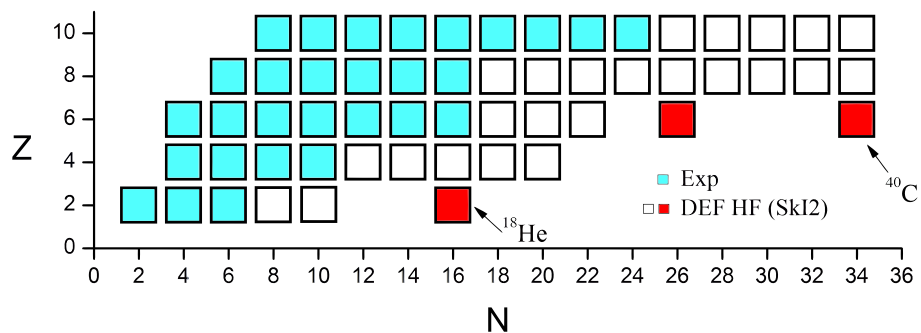


Fig. 1. (Color online). Fragment of NZ chart of even-even nuclei. Empty squares are nuclei stable against one neutron emission in DHF calculations with SkI2 forces. Grey squares represent experimentally known stable nuclei. Black squares are stability peninsulas.

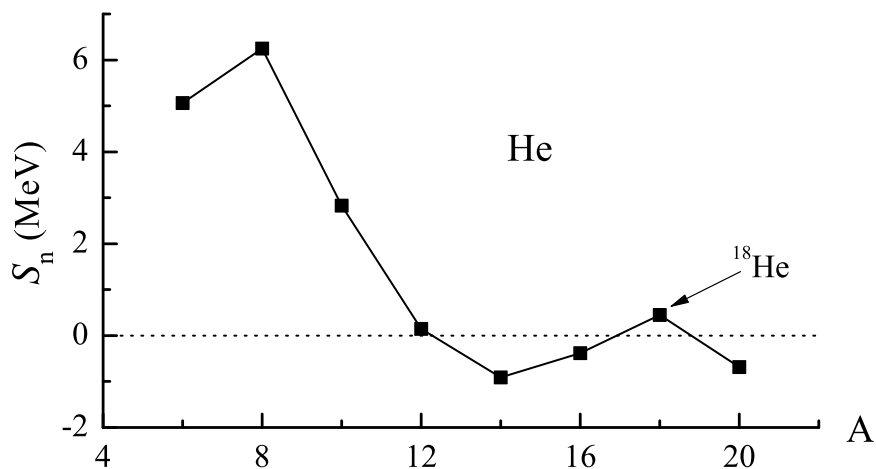


Fig. 2. One neutron separation energies  $S_n$  of helium isotopes as a function of the neutron number obtained in DHF calculations with SkI2 forces. The arrow points at  $^{18}\text{He}$ .

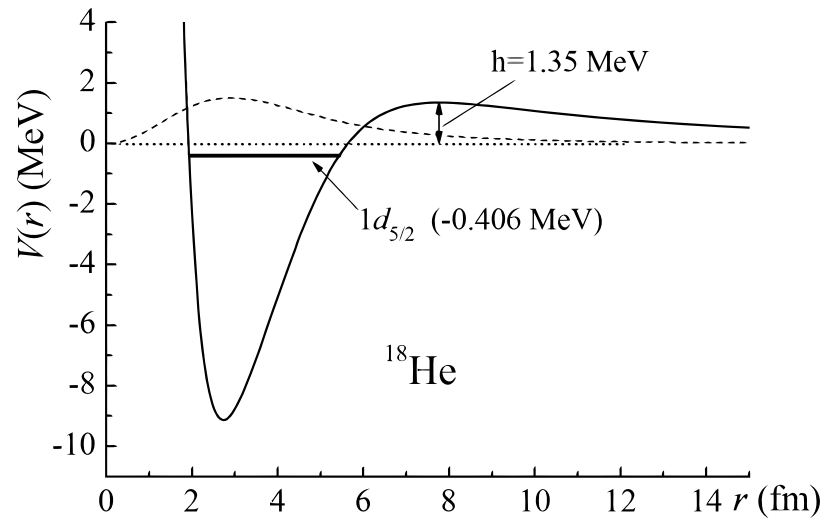


Fig. 3. The last filled level  $1d_{5/2}$  and the corresponding SHF potential  $V(r)$  for  $^{18}\text{He}$  (SkI2 forces). The energy is  $0.406$  MeV, the centrifugal barrier has the height  $1.35$  MeV. The dotted line is the wave function of the level  $1d_{5/2}$ .



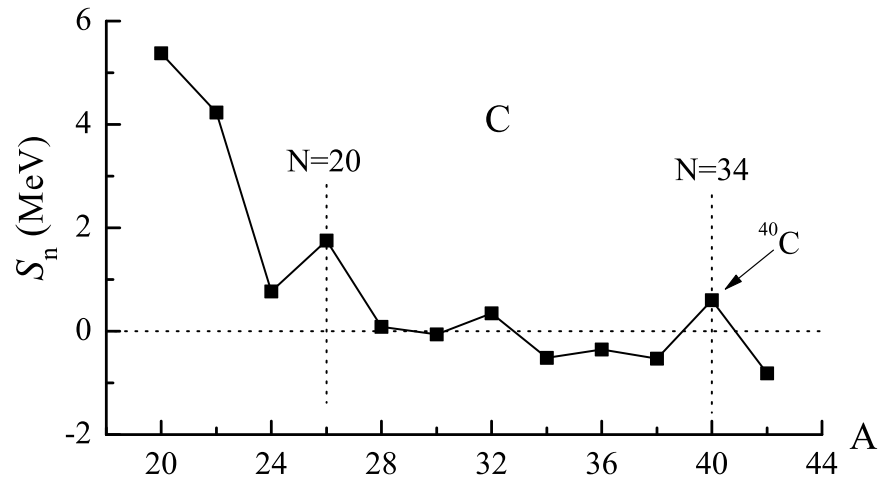


Fig. 4. The same as Fig. 2 but for carbon isotopes. The arrow points at  $^{40}\text{C}$ .

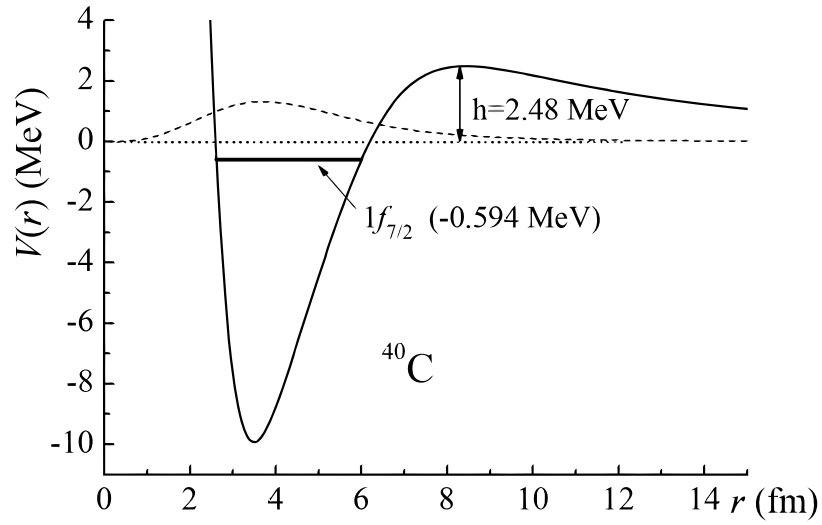


Fig. 5. The last filled level  $1f_{7/2}$  and the corresponding SHF potential  $V(r)$  for  $^{40}\text{C}$  (SkI2 forces). The energy is  $0.594$  MeV, the centrifugal barrier has the height  $2.48$  MeV. The dotted line is the wave function of the level  $1f_{7/2}$ .

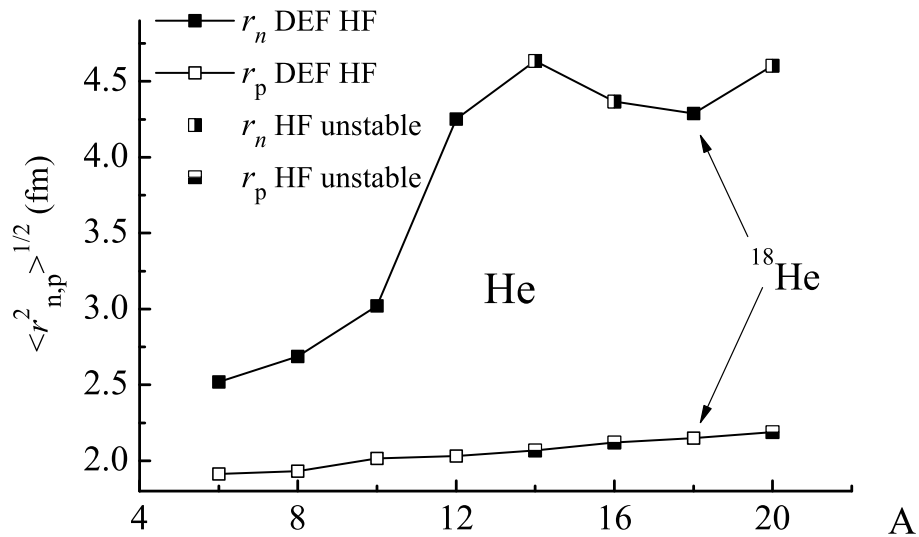


Fig. 6. Neutron (filled squares) and proton (empty squares) root mean square radii of helium isotopes as functions of mass number. These are results of DHF calculations with SkI2 forces. Half-filled squares correspond to nuclei that are unstable against one neutron emission.

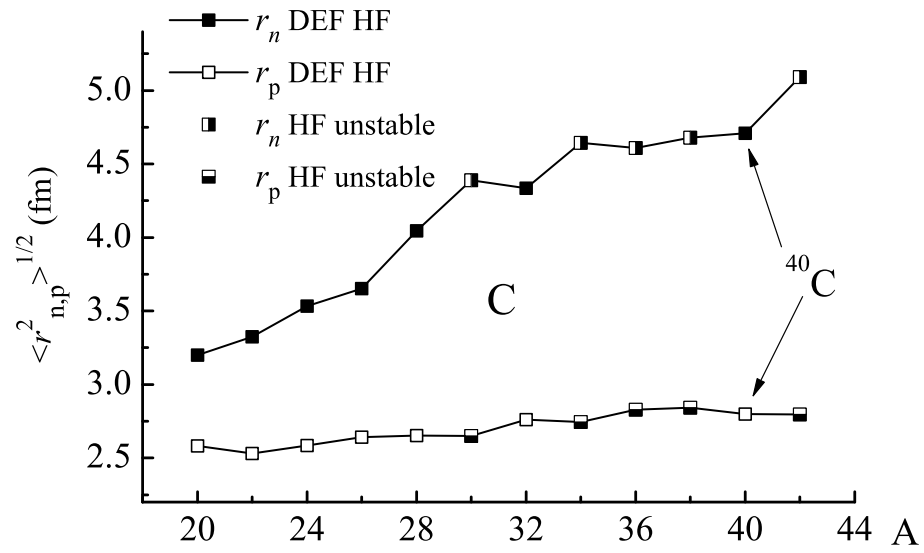


Fig. 7. The same as Fig. 6 but for carbon isotopes.

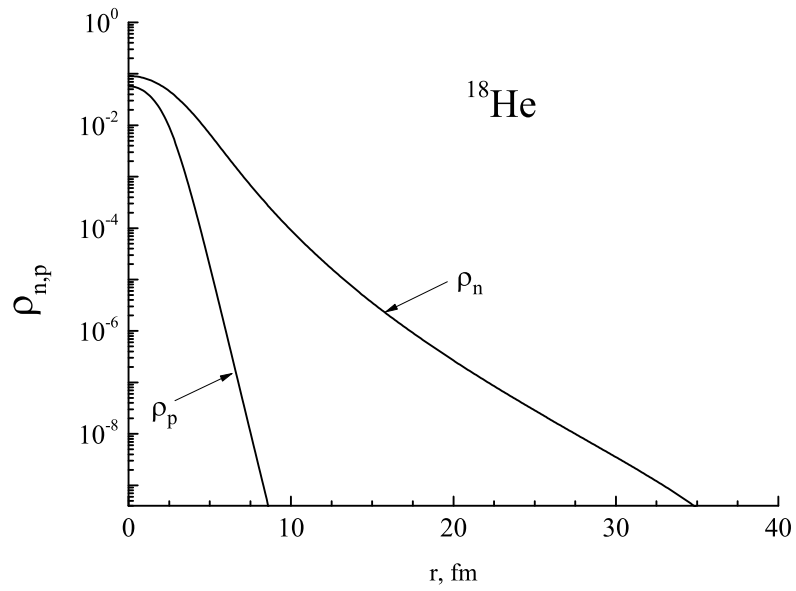


Fig. 8. Neutron and proton density distributions for  $^{18}\text{He}$  calculated within SHF approach with SkI2 forces.

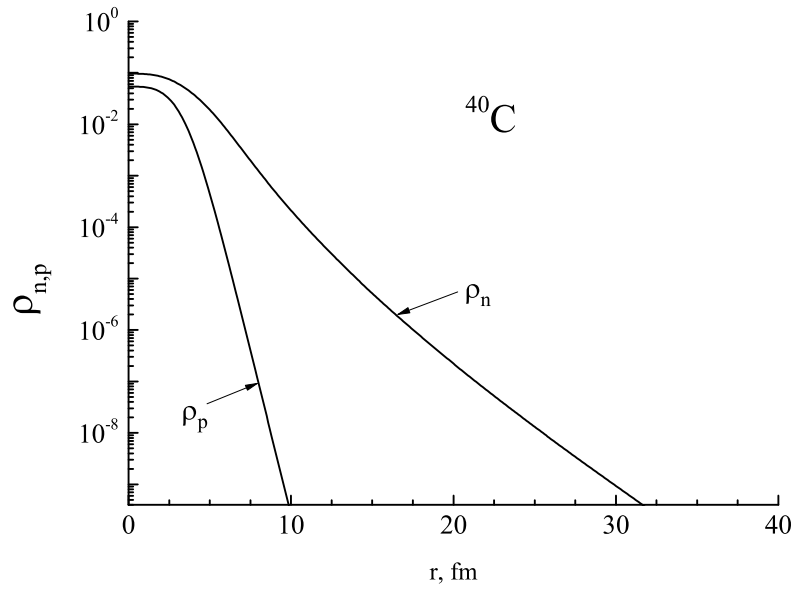


Fig. 9. The same as Fig. 8 but for  $^{40}\text{C}$ .